PERFORMANCE PREDICTION OF HEAT EXCHANGERS
Part III: Effect of Varying the Number of Segmental and Longitudinal Baffles as well as the Number of Tube Passes on the Performance of Shell and Tube Heat Exchangers

Mohamed Khalil Bassiouny
Mechanical Engineering Department, Faculty of Engineering,
University of Menoufia, Shibin El Kom, Egypt.

ABSTRACT

Divided into two major sections, the paper covers a heat transfer analysis of the effect of varying the number of segmental and longitudinal baffles on the total effectiveness of shell and tube heat exchangers in case of a single tube pass as well as double tube passes with different arrangements of inlet and outlet flow ports and under varying the heat capacity rate ratio and the grid effectiveness. The study starts from the separate consideration of reversing the direction of flow on the shell side due to the existence of segmental and longitudinal baffles as well as reversing the direction of the tube side-flow in case of heat exchangers with multi-tube passes. Therefore, a shell and tube heat exchanger can be subdivided at the location of baffles into a set of grids or cells and each of which may be treated as an inferior heat exchanger with crossflow. The results indicate that, in case of a single tube pass, the total effectiveness increases with increasing the number of segmental baffles for counterflow while it increases to approach a limiting value (50%) with three segmental baffles or more for parallel flow. In case of two tube passes, the flow arrangement IV has the optimal effectiveness, whereas the flow type III has the worst one for all number of segmental baffles. It fluctuates between both values, in case of flow arrangements I and II, depending on whether the number of segmental baffles is odd or even. For flow type IV, the effectiveness of a heat exchanger with three segmental baffles is about 10.2% higher than that without baffles. Furthermore, for flow type I and IV, the higher the number of longitudinal baffles the higher the effectiveness of shell and tube heat exchangers. In case of flow types II and III, the effectiveness increases up to three longitudinal baffles then remains unchanged for a single tube pass while for double tube passes, the mounting of longitudinal baffles makes the effectiveness worse and independent of the number of baffles.

INTRODUCTION

A shell and tube heat exchanger, as shown in Figure (1), is built of round tubes mounted in a cylindrical shell with the tube axis parallel to that of the shell. One fluid flows inside the tubes, the other flows across and along the tubes. The major components of this exchanger are tubes (or tube bundle), shell front end head, rear end head, baffles and tubesheets.

Baffles may be classified as segmental (or transverse) and longitudinal types. The purpose of longitudinal baffles is to control the flow direction of the shell fluid such that an overall arrangement of the two fluid streams is achieved.

The classification and application of shell and tube heat exchangers are available in references [1,2]. The newer designs and functional design taking into consideration process variables, utilities and mechanical design are given in [3].

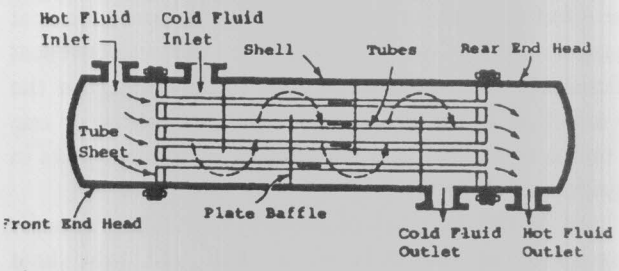

Figure 1. A shell and the tube heat exchanger.

Mikhailov and Özisik [4] developed a finite element method of analysis for heat exchanger calculations. This method is used for computing the temperature distribution and the effectiveness of shell and tube heat exchangers.

Hoffmann [5] and Fanaritis et al [6] presented a design analysis and studied the interdependent parameters involved for developing an optimum unit. By means of computer programs [7], many more parameters that affect flow conditions and heat transfer in a heat exchanger can now be taken into account than was previously possible using manual techniques. In addition, many more configurations may be tried to find a design that satisfies all imposed constraints in the cheapest possible way.

Since in literatures, the baffles in shell and tube heat exchangers are mainly handled as tube supports and there are still no informations about their influence on the performance, the purpose of the present paper is to study the effect of varying the number of segmental and longitudinal baffles on the effectiveness of shell and tube heat exchangers in case of single tube pass and double tube passes for the different possible flow arrangements and under varying both the heat capacity rate ratio and the grid effectiveness.

GRID (CELL) EFFECTIVENESS CONCEPT

A shell and tube heat exchanger can be divided into a set of inferior heat exchangers (cells or grids). This concept starts from the separate consideration of reversing the direction of flow on the shell side due to the existence of segmental and longitudinal baffles as well as reversing the direction of the tube side - flow in case of heat exchangers with multi-tube passes. Each grid or cell may be treated as a sub-heat exchanger with crossflow.

Figure (2-a) represents a shell and tube heat exchanger with six segmental baffles and a single tube pass, while Figure (2-b) shows the equivalent grid arrangement. The corresponding representation for a heat exchanger with one longitudinal baffle is indicated in Figure (3).

The effectiveness of a single grid in a shell and tube heat exchanger, which is necessary for the effectiveness prediction of the whole apparatus, is depending on the flow direction in the grids (either pure crossflow or one side mixed crossflow) and the number of transfer units in the grids as well as the heat capacity rate ratio.

In case of one side mixed crossflow, which is actually taking place in the cells of a shell and tube heat exchanger, the following relation may be applied for predicting the grid effectiveness as given in [8,9].

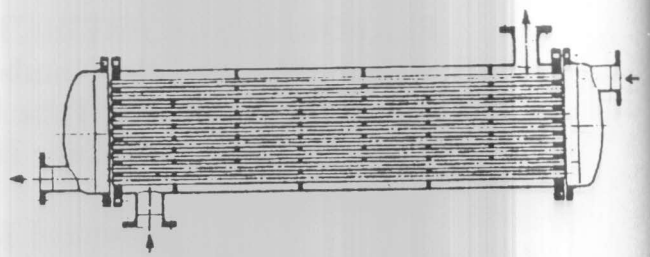

Figure 2-a. A shell and tube heat exchanger with six segmental baffles.

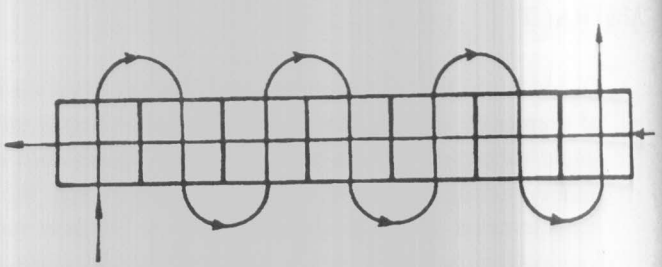

Figure 2-b. Equivalent grid arrangement.

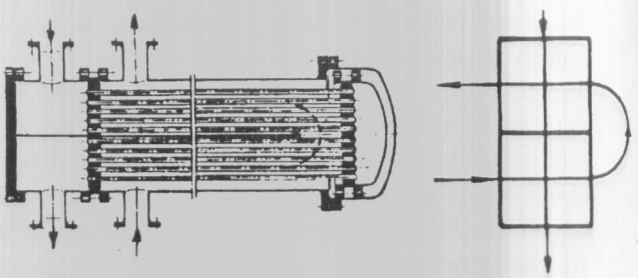

Figure 3. A tube bundle heat exchanger with one longitudinal baffle and the equivalent grid arrangement.

$$\varepsilon_g = \frac{1-\exp\{-C.[1-\exp(-NTU_g)]\}}{C} \qquad (1)$$

VARIATION OF THE NUMBER OF SEGMENTAL BAFFLES

For a shell and tube heat exchanger without longitudinal baffles ($m_l = 0$), the number of segmental baffles (m_s) can be varied along the shell side. Now, the prediction of the heat exchanger effectiveness will be carried out under varying the number of segmental baffles for a single tube pass as well as double tube passes in both cases of cocurrent and counter-current flow regimes.

SINGLE TUBE PASS

One Segmental Baffle

Cocurrent Flow Regime

In this case, the segmental baffle will divide the heat exchanger into two inferior heat exchangers (grids) each with crossflow regime but the two grids are connected together under cocurrent flow condition as indicated in Figure (4).

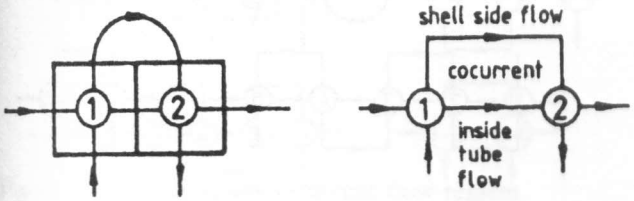

Figure 4. Equivalent grid arrangement of a shell and tube heat exchanger of a single tube pass and one segmental baffle under cocurrent flow regime.

The total effectiveness ε_t of the whole heat exchanger can be calculated making use of the grid effectiveness concept ε_g with the help of eqn.(5) in part I of this work [10]. Therefore, we obtain

$$\varepsilon_t = 2\varepsilon_g - (1 + C).\ \varepsilon_g^2. \tag{2}$$

Counter-Current Flow Regime

The total effectiveness of the counterflow heat exchanger considered, see Figure (5), can be obtained from eqn.(22) in part I of this study [10] using the grid effectiveness concept as follows:

$$\varepsilon_t = \frac{2\varepsilon_g - (1+C).\varepsilon_g^2}{1 - C.\varepsilon_g^2} = 1 - \frac{(1-\varepsilon_g)^2}{1 - C.\varepsilon_g^2}. \tag{3}$$

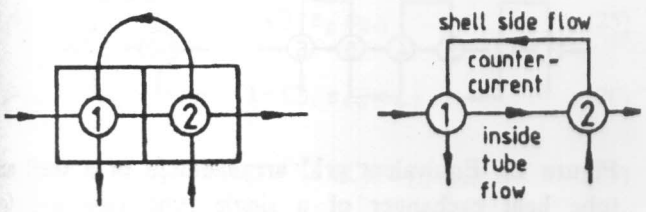

Figure 5. Case of counter-current flow regime.

In a similar way, the total effectiveness of shell and tube heat exchangers under variation of the number of segmental baffles can be calculated by subdividing the heat exchanger into cells (inferior heat exchangers), as illustrated above, and then combining each pair of grids together in cocurrent or counter-current flow regimes using eqn.(2) or eqn.(3) respectively to determine an equivalent effectiveness for each pair. This combination method is repeated until reaching the total effectiveness of the whole heat exchanger. The calculation procedure is explained by the following figures and equations for different number of segmental baffles:

Two Segmental Baffles
Cocurrent Flow Regime

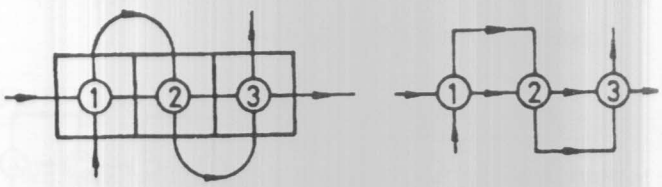

Figure 6. Equivalent grid arrangement of a shell and tube heat exchanger of a single tube pass and two segmental baffles under cocurrent flow regime.

$$\varepsilon_{2\text{-}3} = 2\varepsilon_g - (1+C).\varepsilon_g^2 \tag{4}$$

$$\varepsilon_t = \varepsilon_{1\text{-}3} = \varepsilon_g + \varepsilon_{2\text{-}3} - (1+C).\ \varepsilon_g\ \varepsilon_{2\text{-}3}. \tag{5}$$

Counter-Current Flow Regime

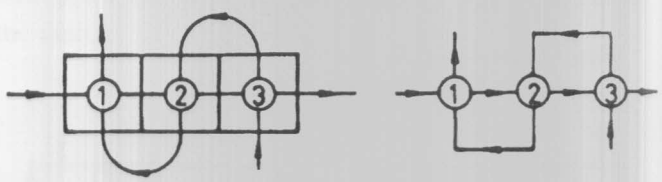

Figure 7. Case of counter-current flow regime.

$$\varepsilon_{2\text{-}3} = 1 - \frac{(1-\varepsilon_g)^2}{1 - C.\varepsilon_g^2} \tag{6}$$

$$\varepsilon_t = \varepsilon_{1\text{-}3} = \frac{\varepsilon_g + \varepsilon_{2\text{-}3} - (1+C).\varepsilon_g\varepsilon_{2\text{-}3}}{1 - C\varepsilon_g\varepsilon_{2\text{-}3}} \tag{7}$$

Three Segmental Baffles
Cocurrent Flow Regime

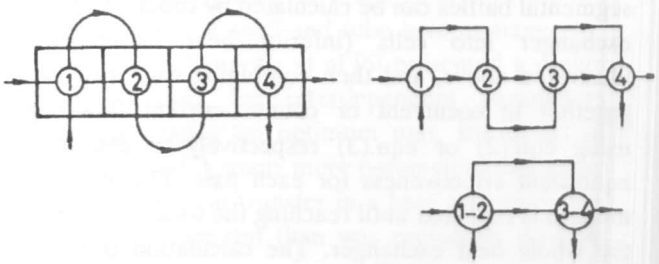

Figure 8. Equivalent grid arrangement of a shell and tube heat exchanger of a single tube pass and three segmental baffles under cocurrent flow regime.

$$\varepsilon_{1-2} = \varepsilon_{3-4} = 2\varepsilon_g - (1+C).\ \varepsilon_g^2 \tag{8}$$

$$\varepsilon_t = \varepsilon_{1-4} = \varepsilon_{1-2} + \varepsilon_{3-4} - (1+C).\ \varepsilon_{1-2}\ \varepsilon_{3-4} \tag{9}$$

Counter-Current Flow Regime

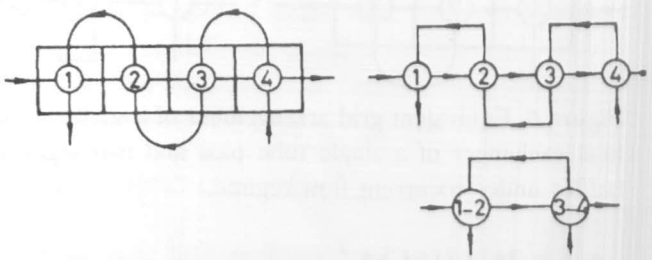

Figure 9. Case of counter-current flow regiem.

$$\varepsilon_{1-2} = \varepsilon_{3-4} = 1 - \frac{(1-\varepsilon_g)^2}{1-C.\varepsilon_g^2} \tag{10}$$

$$\varepsilon_t = \varepsilon_{1-4} = \frac{\varepsilon_{1-2} + \varepsilon_{3-4} - (1+C).\varepsilon_{1-2}\varepsilon_{3-4}}{1-C.\varepsilon_{1-2}\varepsilon_{3-4}} \tag{11}$$

Four Segmental Baffles
Cocurrent Flow Regime

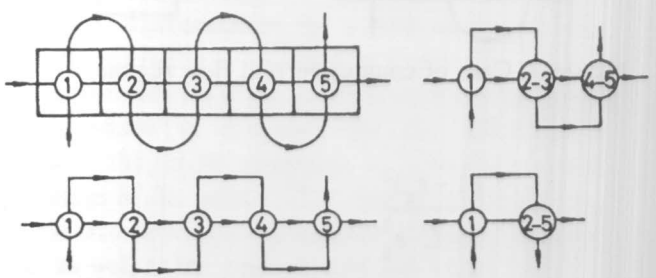

Figure 10. Equivalent grid arrangement of a shell and tube heat exchanger of a single tube pass and four segmental baffles under cocurrent flow regime.

$$\varepsilon_{2-3} = \varepsilon_{4-5} = 2\varepsilon_g - (1+C).\ \varepsilon_g^2 \tag{12}$$

$$\varepsilon_{2-5} = \varepsilon_{2-3} + \varepsilon_{4-5} - (1+C).\ \varepsilon_{2-3}\ \varepsilon_{4-5} \tag{13}$$

$$\varepsilon_t = \varepsilon_{1-5} = \varepsilon_g + \varepsilon_{2-5} - (1+C).\ \varepsilon_g\ \varepsilon_{2-5}. \tag{14}$$

Counter-Current Flow Regime

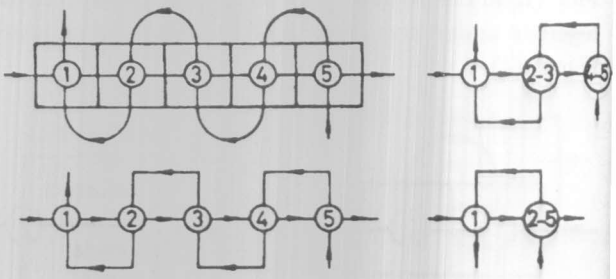

Figure 11. Case of counter-current flow regiem.

$$\varepsilon_{2-3} = \varepsilon_{4-5} = 1 - \frac{(1-\varepsilon_g)^2}{1-C.\varepsilon_g^2} \tag{15}$$

$$\varepsilon_{2-5} = \frac{\varepsilon_{2-3} + \varepsilon_{4-5} - (1+C).\varepsilon_{2-3}\varepsilon_{4-5}}{1-C.\varepsilon_{2-3}\varepsilon_{4-5}} \tag{16}$$

$$\varepsilon_t = \varepsilon_{1-5} = \frac{\varepsilon_g + \varepsilon_{2-5} - (1+C).\varepsilon_g\,\varepsilon_{2-5}}{1-C.\varepsilon_g\,\varepsilon_{2-5}} \tag{17}$$

Five Segmental Baffles

Cocurrent Flow Regime

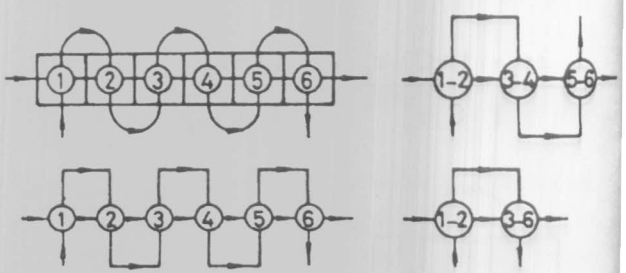

Figure 12. Equivalent grid arrangement of a shell and tube heat exchanger of a single tube pass and five segmental baffles under cocurrent flow regime.

DOUBLE TUBE PASSES

One Segmental Baffle
Flow Arrangement I

$$\varepsilon_{1-2} = 1 - \frac{(1-\varepsilon_g)^2}{1-C.\varepsilon_g^2} \tag{32}$$

$$\varepsilon_{1-3} = \frac{\varepsilon_{1-2} + \varepsilon_g - (1+C).\varepsilon_{1-2}\,\varepsilon_g}{1-C.\varepsilon_{1-2}\,\varepsilon_g} \tag{33}$$

$$\varepsilon_t = \varepsilon_{1-4} = \varepsilon_{1-3} + \varepsilon_g - (1+C).\,\varepsilon_{1-3}\,\varepsilon_g \tag{34}$$

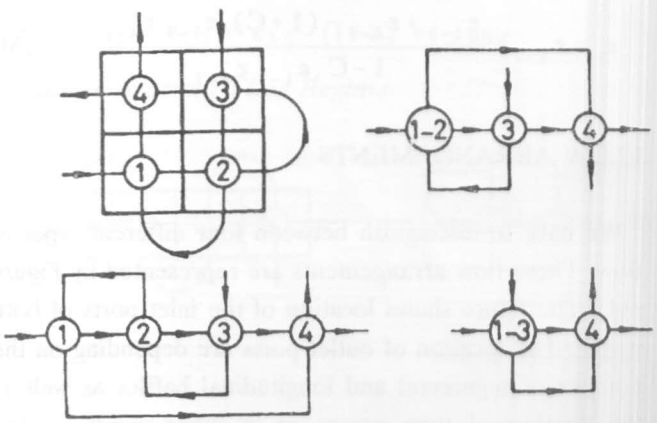

Figure 15. Equivalent grid arrangement of a shell and tube heat exchanger of double tube passes and one segmental baffle, in case of flow arrangement I.

Flow Arrangement II

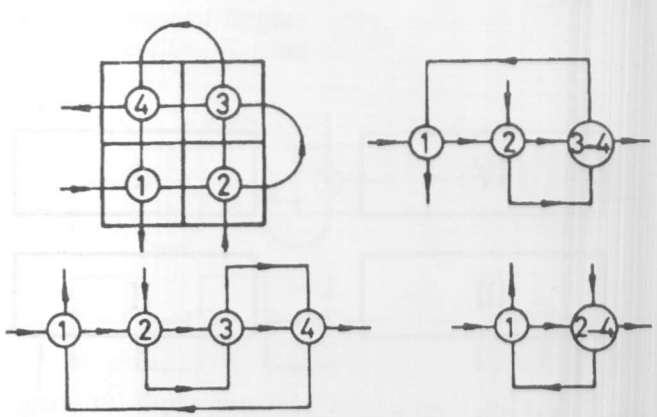

Figure 16. Case of flow arrangement II.

$$\varepsilon_{3-4} = 2\varepsilon_g - (1+C).\,\varepsilon_g^2 \tag{35}$$

$$\varepsilon_{2-4} = \varepsilon_g + \varepsilon_{3-4} - (1+C).\,\varepsilon_g\,\varepsilon_{3-4} \tag{36}$$

$$\varepsilon_t = \varepsilon_{1-4} = \frac{\varepsilon_g + \varepsilon_{2-4} - (1+C).\,\varepsilon_g\,\varepsilon_{2-4}}{1-C.\,\varepsilon_g\,\varepsilon_{2-4}} \tag{37}$$

Flow Arrangement III

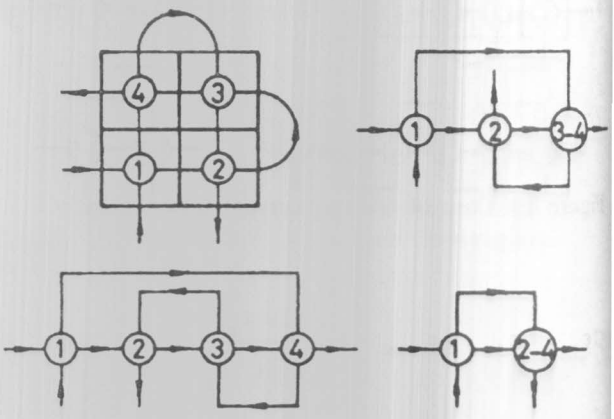

Figure 17. Case of flow arrangement III.

$$\varepsilon_{3-4} = 1 - \frac{(1-\varepsilon_g)^2}{1-C.\varepsilon_g^2} \tag{38}$$

$$\varepsilon_{2-4} = \frac{\varepsilon_g + \varepsilon_{3-4} - (1+C).\,\varepsilon_g\,\varepsilon_{3-4}}{1-C.\,\varepsilon_g\,\varepsilon_{3-4}} \tag{39}$$

$$\varepsilon_t = \varepsilon_{1-4} = \varepsilon_g + \varepsilon_{2-4} - (1+C).\,\varepsilon_g\,\varepsilon_{2-4}. \tag{40}$$

Flow Arrangement IV

$$\varepsilon_{1-2} = 2\varepsilon_g - (1+C).\,\varepsilon_g^2 \tag{41}$$

$$\varepsilon_{1-3} = \varepsilon_{1-2} + \varepsilon_g - (1+C).\,\varepsilon_{1-2}\,\varepsilon_g \tag{42}$$

$$\varepsilon_t = \varepsilon_{1-4} = \frac{\varepsilon_{1-3} + \varepsilon_g - (1+C).\,\varepsilon_{1-3}\,\varepsilon_g}{1-C.\,\varepsilon_{1-3}\,\varepsilon_g} \tag{43}$$

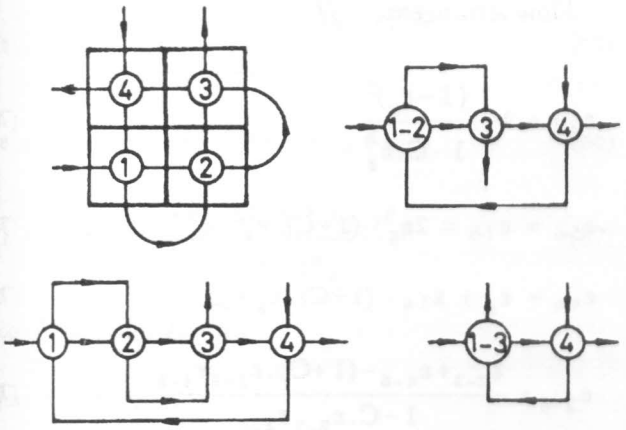

Figure 18. Case of flow arrangement IV.

Two Segmental Baffles
Flow Arrangement I

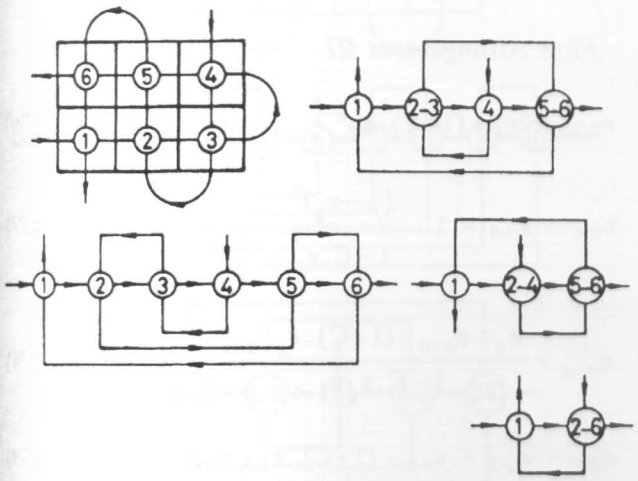

Figure 19. Equivalent grid arrangement of double tube passes and two segmental baffles, in case of flow arrangement I.

$$\varepsilon_{2-3} = 1 - \frac{(1-\varepsilon_g)^2}{1-C.\varepsilon_g^2} \tag{44}$$

$$\varepsilon_{5-6} = 2\varepsilon_g - (1+C).\ \varepsilon_g^{\,2} \tag{45}$$

$$\varepsilon_{2-4} = \frac{\varepsilon_{2-3} + \varepsilon_g - (1+C).\varepsilon_{2-3}\varepsilon_g}{1-C.\varepsilon_{2-3}\varepsilon_g} \tag{46}$$

$$\varepsilon_{2-6} = \varepsilon_{2-4} + \varepsilon_{5-6} - (1+C).\ \varepsilon_{2-4}\ \varepsilon_{5-6} \tag{47}$$

$$\varepsilon_t = \varepsilon_{1-6} = \frac{\varepsilon_g + \varepsilon_{2-6} - (1+C).\varepsilon_g\varepsilon_{2-6}}{1-C.\varepsilon_g\varepsilon_{2-6}} \tag{48}$$

Flow Arrangement II

$$\varepsilon_{1-2} = 1 - \frac{(1-\varepsilon_g)^2}{1-C.\varepsilon_g^2} \tag{49}$$

$$\varepsilon_{4-5} = 2\varepsilon_g - (1+C).\ \varepsilon_g^{\,2} \tag{50}$$

$$\varepsilon_{3-5} = \varepsilon_g + \varepsilon_{4-5} - (1+C).\ \varepsilon_g\ \varepsilon_{4-5} \tag{51}$$

$$\varepsilon_{1-5} = \frac{\varepsilon_{1-2} + \varepsilon_{3-5} - (1+C).\varepsilon_{1-2}\varepsilon_{3-5}}{1-C.\varepsilon_{1-2}\varepsilon_{3-5}} \tag{52}$$

$$\varepsilon_t = \varepsilon_{1-6} = \varepsilon_{1-5} + \varepsilon_g - (1+C).\ \varepsilon_{1-5}\ \varepsilon_g. \tag{53}$$

Flow Arrangement III

$$\varepsilon_{2-3} = 2\varepsilon_g - (1+C).\ \varepsilon_g^{\,2} \tag{54}$$

$$\varepsilon_{5-6} = 1 - \frac{(1-\varepsilon_g)^2}{1-C.\varepsilon_g^2} \tag{55}$$

$$\varepsilon_{2-4} = \varepsilon_{2-3} + \varepsilon_g - (1+C).\ \varepsilon_{2-3}\ \varepsilon_g \tag{56}$$

$$\varepsilon_{2-6} = \frac{\varepsilon_{2-4} + \varepsilon_{5-6} - (1+C).\varepsilon_{2-4}\varepsilon_{5-6}}{1-C.\varepsilon_{2-4}\varepsilon_{5-6}} \tag{57}$$

$$\varepsilon_t = \varepsilon_{1-6} = \varepsilon_g + \varepsilon_{2-6} - (1+C).\ \varepsilon_g\ \varepsilon_{2-6}. \tag{58}$$

Flow Arrangement IV

$$\varepsilon_{1-2} = 2\varepsilon_g - (1+C).\ \varepsilon_g^{\,2} \tag{59}$$

$$\varepsilon_{4-5} = 1 - \frac{(1-\varepsilon_g)^2}{1-C.\varepsilon_g^2} \tag{60}$$

$$\varepsilon_{3-5} = \frac{\varepsilon_g + \varepsilon_{4-5} - (1+C).\varepsilon_g\varepsilon_{4-5}}{1-C.\varepsilon_g\varepsilon_{4-5}} \tag{61}$$

$$\varepsilon_{1-5} = \varepsilon_{1-2} + \varepsilon_{3-5} - (1+C).\ \varepsilon_{1-2}\ \varepsilon_{3-5} \tag{62}$$

$$\varepsilon_t = \varepsilon_{1-6} = \frac{\varepsilon_{1-5} + \varepsilon_g - (1+C).\varepsilon_{1-5}\varepsilon_g}{1 - C.\varepsilon_{1-5}\varepsilon_g} \quad (63)$$

Three Segmental Baffles
Flow Arrangement I

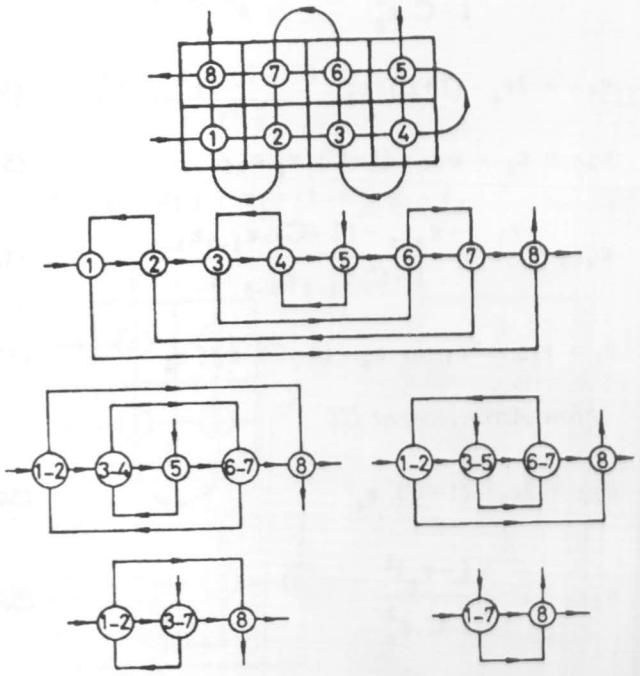

Figure 20. Equivalent grid arrangement of a double tube passes and three segmental baffles, in case of flow arrangement I.

$$\varepsilon_{1-2} = \varepsilon_{3-4} = 1 - \frac{(1-\varepsilon_g)^2}{1 - C.\varepsilon_g^2} \quad (64)$$

$$\varepsilon_{6-7} = 2\varepsilon_g - (1+C).\varepsilon_g^2 \quad (65)$$

$$\varepsilon_{3-5} = \frac{\varepsilon_{3-4} + \varepsilon_g - (1+C).\varepsilon_{3-4}\varepsilon_g}{1 - C.\varepsilon_{3-4}\varepsilon_g} \quad (66)$$

$$\varepsilon_{3-7} = \varepsilon_{3-5} + \varepsilon_{6-7} - (1+C).\varepsilon_{3-5}\varepsilon_{6-7} \quad (67)$$

$$\varepsilon_{1-7} = \frac{\varepsilon_{1-2} + \varepsilon_{3-7} - (1+C).\varepsilon_{1-2}\varepsilon_{3-7}}{1 - C.\varepsilon_{1-2}\varepsilon_{3-7}} \quad (68)$$

$$\varepsilon_t = \varepsilon_{1-8} = \varepsilon_{1-7} + \varepsilon_g - (1+C).\varepsilon_{1-7}\varepsilon_g \quad (69)$$

Flow Arrangement II

$$\varepsilon_{2-3} = 1 - \frac{(1-\varepsilon_g)^2}{1 - C.\varepsilon_g^2} \quad (70)$$

$$\varepsilon_{5-6} = \varepsilon_{7-8} = 2\varepsilon_g - (1+C).\varepsilon_g^2 \quad (71)$$

$$\varepsilon_{4-6} = \varepsilon_g + \varepsilon_{5-6} - (1+C).\varepsilon_g\varepsilon_{5-6} \quad (72)$$

$$\varepsilon_{2-6} = \frac{\varepsilon_{2-3} + \varepsilon_{4-6} - (1+C).\varepsilon_{2-3}\varepsilon_{4-6}}{1 - C.\varepsilon_{2-3}\varepsilon_{4-6}} \quad (73)$$

$$\varepsilon_{2-8} = \varepsilon_{2-6} + \varepsilon_{7-8} - (1+C).\varepsilon_{2-6}\varepsilon_{7-8} \quad (74)$$

$$\varepsilon_t = \varepsilon_{1-8} = \frac{\varepsilon_g + \varepsilon_{2-8} - (1+C).\varepsilon_g\varepsilon_{2-8}}{1 - C.\varepsilon_g\varepsilon_{2-8}} \quad (75)$$

Flow Arrangement III

$$\varepsilon_{2-3} = 2\varepsilon_g - (1+C).\varepsilon_g^2 \quad (76)$$

$$\varepsilon_{5-6} = \varepsilon_{7-8} = 1 - \frac{(1-\varepsilon_g)^2}{1 - C.\varepsilon_g^2} \quad (77)$$

$$\varepsilon_{4-6} = \frac{\varepsilon_g + \varepsilon_{5-6} - (1+C).\varepsilon_g\varepsilon_{5-6}}{1 - C.\varepsilon_g\varepsilon_{5-6}} \quad (78)$$

$$\varepsilon_{2-6} = \varepsilon_{2-3} + \varepsilon_{4-6} - (1+C).\varepsilon_{2-3}\varepsilon_{4-6} \quad (79)$$

$$\varepsilon_{2-8} = \frac{\varepsilon_{2-6} + \varepsilon_{7-8} - (1+C).\varepsilon_{2-6}\varepsilon_{7-8}}{1 - C.\varepsilon_{2-6}\varepsilon_{7-8}} \quad (80)$$

$$\varepsilon_t = \varepsilon_{1-8} = \varepsilon_g + \varepsilon_{2-8} - (1+C).\varepsilon_g\varepsilon_{2-8}. \quad (81)$$

Flow Arrangement IV

$$\varepsilon_{1-2} = \varepsilon_{3-4} = 2\varepsilon_g - (1+C).\varepsilon_g^2 \quad (82)$$

$$\varepsilon_{6-7} = 1 - \frac{(1-\varepsilon_g)^2}{1 - C.\varepsilon_g^2} \quad (83)$$

$$\varepsilon_{3-5} = \varepsilon_{3-4} + \varepsilon_g - (1+C).\varepsilon_{3-4}\varepsilon_g \quad (84)$$

$$\varepsilon_{3-7}=\frac{\varepsilon_{3-5}+\varepsilon_{6-7}-(1+C).\varepsilon_{3-5}\varepsilon_{6-7}}{1-C.\varepsilon_{3-5}\varepsilon_{6-7}} \quad (85)$$

$$\varepsilon_{1-7} = \varepsilon_{1-2} + \varepsilon_{3-7} - (1+C).\ \varepsilon_{1-2}\ \varepsilon_{3-7} \quad (86)$$

$$\varepsilon_t=\varepsilon_{1-8}=\frac{\varepsilon_{1-7}+\varepsilon_g-(1+C).\varepsilon_{1-7}\varepsilon_g}{1-C.\varepsilon_{1-7}\varepsilon_g} \quad (87)$$

Four Segmental Baffles

Flow Arrangement I

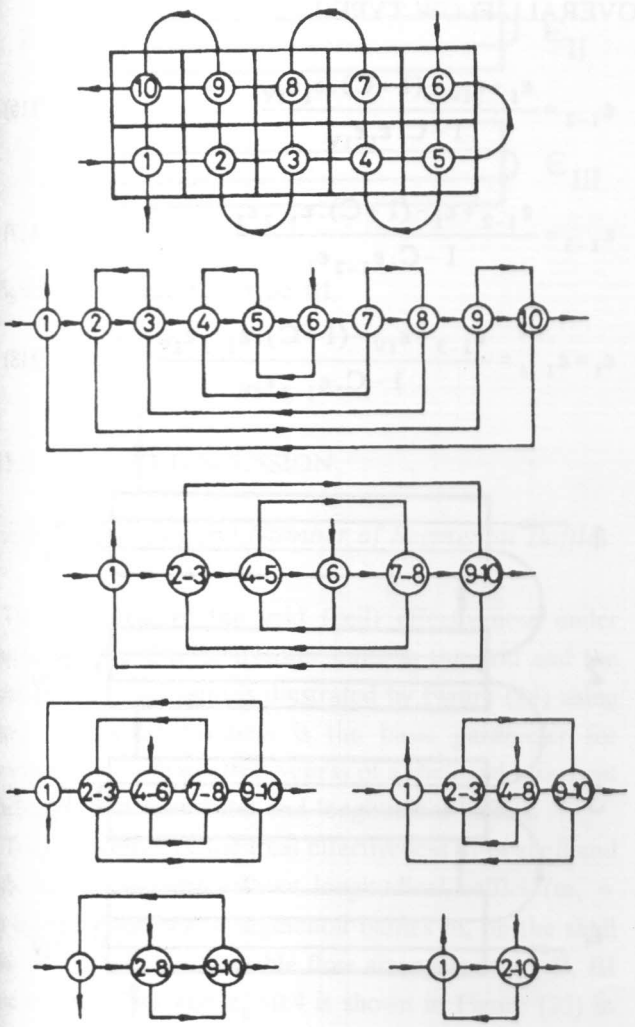

Figure 21. Equivalent grid arrangement of a shell and tube heat exchanger of double tube passes and four segmental baffles, in case of flow arrangement I.

$$\varepsilon_{2-3}=\varepsilon_{4-5}=1-\frac{(1-\varepsilon_g)^2}{1-C.\varepsilon_g^2} \quad (88)$$

$$\varepsilon_{7-8} = \varepsilon_{9-10} = 2\varepsilon_g - (1+C).\ \varepsilon_g^{\,2} \quad (89)$$

$$\varepsilon_{4-6}=\frac{\varepsilon_{4-5}+\varepsilon_g-(1+C).\varepsilon_{4-5}\varepsilon_g}{1-C.\varepsilon_{4-5}\varepsilon_g} \quad (90)$$

$$\varepsilon_{4-8} = \varepsilon_{4-6} + \varepsilon_{7-8} - (1+C).\ \varepsilon_{4-6}\ \varepsilon_{7-8} \quad (91)$$

$$\varepsilon_{2-8}=\frac{\varepsilon_{2-3}+\varepsilon_{4-8}-(1+C).\varepsilon_{2-3}\varepsilon_{4-8}}{1-C.\varepsilon_{2-3}\varepsilon_{4-8}} \quad (92)$$

$$\varepsilon_{2-10} = \varepsilon_{2-8} + \varepsilon_{9-10} - (1+C).\ \varepsilon_{2-8}\ \varepsilon_{9-10} \quad (93)$$

$$\varepsilon_t=\varepsilon_{1-10}=\frac{\varepsilon_g+\varepsilon_{2-10}-(1+C).\varepsilon_g\varepsilon_{2-10}}{1-C.\varepsilon_g\varepsilon_{2-10}} \quad (94)$$

Flow Arrangement II

$$\varepsilon_{1-2}=\varepsilon_{3-4}=1-\frac{(1-\varepsilon_g)^2}{1-C.\varepsilon_g^2} \quad (95)$$

$$\varepsilon_{6-7} = \varepsilon_{8-9} = 2\varepsilon_g - (1+C).\ \varepsilon_g^{\,2} \quad (96)$$

$$\varepsilon_{5-7} = \varepsilon_g + \varepsilon_{6-7} - (1+C).\ \varepsilon_g\ \varepsilon_{6-7} \quad (97)$$

$$\varepsilon_{3-7}=\frac{\varepsilon_{3-4}+\varepsilon_{5-7}-(1+C).\varepsilon_{3-4}\varepsilon_{5-7}}{1-C.\varepsilon_{3-4}\varepsilon_{5-7}} \quad (98)$$

$$\varepsilon_{3-9} = \varepsilon_{3-7} + \varepsilon_{8-9} - (1+C).\ \varepsilon_{3-7}\ \varepsilon_{8-9} \quad (99)$$

$$\varepsilon_{1-9}=\frac{\varepsilon_{1-2}+\varepsilon_{3-9}-(1+C).\varepsilon_{1-2}\varepsilon_{3-9}}{1-C.\varepsilon_{1-2}\varepsilon_{3-9}} \quad (100)$$

$$\varepsilon_t = \varepsilon_{1-10} = \varepsilon_{1-9} + \varepsilon_g - (1+C).\ \varepsilon_{1-9}\ \varepsilon_g \quad (101)$$

Flow Arrangement III

$$\varepsilon_{2-3} = \varepsilon_{4-5} = 2\varepsilon_g - (1+C).\ \varepsilon_g^{\,2} \quad (102)$$

$$\varepsilon_{7-8} = \varepsilon_{9-10} = 1 - \frac{(1-\varepsilon_g)^2}{1 - C.\varepsilon_g^2} \quad (103)$$

$$\varepsilon_{4-6} = \varepsilon_{4-5} + \varepsilon_g - (1+C).\ \varepsilon_{4-5}\ \varepsilon_g \quad (104)$$

$$\varepsilon_{4-8} = \frac{\varepsilon_{4-6} + \varepsilon_{7-8} - (1+C).\varepsilon_{4-6}\varepsilon_{7-8}}{1 - C.\varepsilon_{4-6}\varepsilon_{7-8}} \quad (105)$$

$$\varepsilon_{2-8} = \varepsilon_{2-3} + \varepsilon_{4-8} - (1+C).\ \varepsilon_{2-3}\ \varepsilon_{4-8} \quad (106)$$

$$\varepsilon_{2-10} = \frac{\varepsilon_{2-8} + \varepsilon_{9-10} - (1+C).\varepsilon_{2-8}\varepsilon_{9-10}}{1 - C.\varepsilon_{2-8}\varepsilon_{9-10}} \quad (107)$$

$$\varepsilon_t = \varepsilon_{1-10} = \varepsilon_g + \varepsilon_{2-10} - (1+C).\ \varepsilon_g\ \varepsilon_{2-10} \quad (108)$$

Flow Arrangement IV

$$\varepsilon_{1-2} = \varepsilon_{3-4} = 2\varepsilon_g - (1+C).\ \varepsilon_g^2 \quad (109)$$

$$\varepsilon_{6-7} = \varepsilon_{8-9} = 1 - \frac{(1-\varepsilon_g)^2}{1 - C.\varepsilon_g^2} \quad (110)$$

$$\varepsilon_{5-7} = \frac{\varepsilon_g + \varepsilon_{6-7} - (1+C).\varepsilon_g\varepsilon_{6-7}}{1 - C.\varepsilon_g\varepsilon_{6-7}} \quad (111)$$

$$\varepsilon_{3-7} = \varepsilon_{3-4} + \varepsilon_{5-7} - (1+C).\ \varepsilon_{3-4}\ \varepsilon_{5-7} \quad (112)$$

$$\varepsilon_{3-9} = \frac{\varepsilon_{3-7} + \varepsilon_{8-9} - (1+C).\varepsilon_{3-7}\varepsilon_{8-9}}{1 - C.\varepsilon_{3-7}\varepsilon_{8-9}} \quad (113)$$

$$\varepsilon_{1-9} = \varepsilon_{1-2} + \varepsilon_{3-9} - (1+C).\ \varepsilon_{1-2}\ \varepsilon_{3-9} \quad (114)$$

$$\varepsilon_t = \varepsilon_{1-10} = \frac{\varepsilon_{1-9} + \varepsilon_g - (1+C).\varepsilon_{1-9}\varepsilon_g}{1 - C.\varepsilon_{1-9}\varepsilon_g} \quad (115)$$

VARIATION OF THE NUMBER OF LONGITUDINAL BAFFLES

In this case, the heat exchanger can be divided into a set of sub-heat exchangers at the location of the longitudinal baffles. The number of these exchangers will be equal to $(m_t + 1)$. For overall flow types I and IV, the sub-heat exchangers will be arranged in counter-current flow regime while for overall flow type II and III they are connected in cocurrent flow regime. The individual effectiveness of each sub-heat exchanger is depending on the number of segmental baffles and the number of tube passes as well as its individual flow type.

For the sake of shortness, only two overall flow arrangements I and III with three longitudinal baffles will be discussed in this section but the results will be extended to cover all flow types under varying the number of longitudinal baffles in the heat exchangers, the number of segmental baffles and the number of inside tube - passes in each sub-heat exchanger.

OVERALL FLOW TYPE I

$$\varepsilon_{1-2} = \frac{\varepsilon_I + \varepsilon_{IV} - (1+C).\varepsilon_I\varepsilon_{IV}}{1 - C.\varepsilon_I\varepsilon_{IV}} \quad (116)$$

$$\varepsilon_{1-3} = \frac{\varepsilon_{1-2} + \varepsilon_I - (1+C).\varepsilon_{1-2}\varepsilon_I}{1 - C.\varepsilon_{1-2}\varepsilon_I} \quad (117)$$

$$\varepsilon_t = \varepsilon_{1-4} = \frac{\varepsilon_{1-3} + \varepsilon_{IV} - (1+C).\varepsilon_{1-3}\varepsilon_{IV}}{1 - C.\varepsilon_{1-3}\varepsilon_{IV}} \quad (118)$$

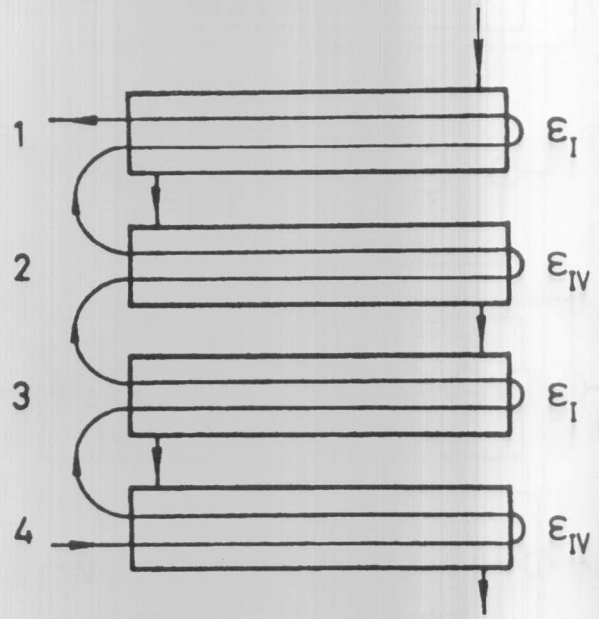

Figure 22. Overall flow type I.

OVERALL FLOW TYPE III

$$\varepsilon_{1-2} = \varepsilon_{III} + \varepsilon_{II} - (1+C).\ \varepsilon_{III}\ \varepsilon_{II} \quad (119)$$

$$\varepsilon_{1-3} = \varepsilon_{1-2} + \varepsilon_{III} - (1+C).\ \varepsilon_{1-2}\ \varepsilon_{III} \quad (120)$$

$$\varepsilon_t = \varepsilon_{1-4} = \varepsilon_{1-3} + \varepsilon_{II} - (1+C).\ \varepsilon_{1-3}\ \varepsilon_{II} \quad (121)$$

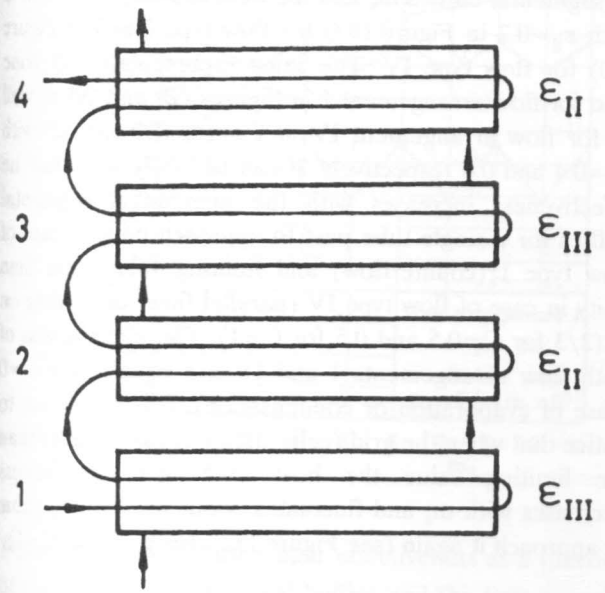

Figure 23. Overall flow type III.

RESULTS AND DISCUSSION

Effect of Varying the Number of Segmental Baffles

The behaviour of the grid (cell) effectiveness under varying the number of transfer units in the grid and the heat capacity rate ratio is illustrated by Figure (24) using eqn.(1). This effectiveness is the basic parameter for predicting the overall effectiveness of a shell and tube heat exchanger with segmental and longitudinal baffles.

The dependence of the total effectiveness ε_t of shell and tube heat exchangers without longitudinal baffles (m_t = 0) upon the number of segmental baffles m_s on the shell side for the different possible flow arrangements I, II, III and IV with C=1 and ε_g=0.4 is shown in Figure (25) in case of a single tube pass and in Figure (26) in case of double tube passes. It is clear that, in case of a single tube pass, the total effectiveness increases always with increasing the number of segmental baffles for flow types I and II which represent counter-current flow regimes while it increases to approach a limiting value (50%) when $m_s \geq 3$ for flow types III and IV (cases of cocurrent flow regime).

In case of double tube passes, the flow arrangement IV has the optimal effectiveness while the flow type III has the worst one for both odd and even number of segmental baffles. It fluctuates between both effectivenesses in case of flow arrangements I and II depending on whether the number of segmental baffles is even or odd. For flow type IV, the effectiveness increases from 57.14% in case of a heat exchanger without segmental baffles to 62.96% in case of a heat exchanger with 3 segmental baffles or more which means an increase of about 10.2% in the effectiveness.

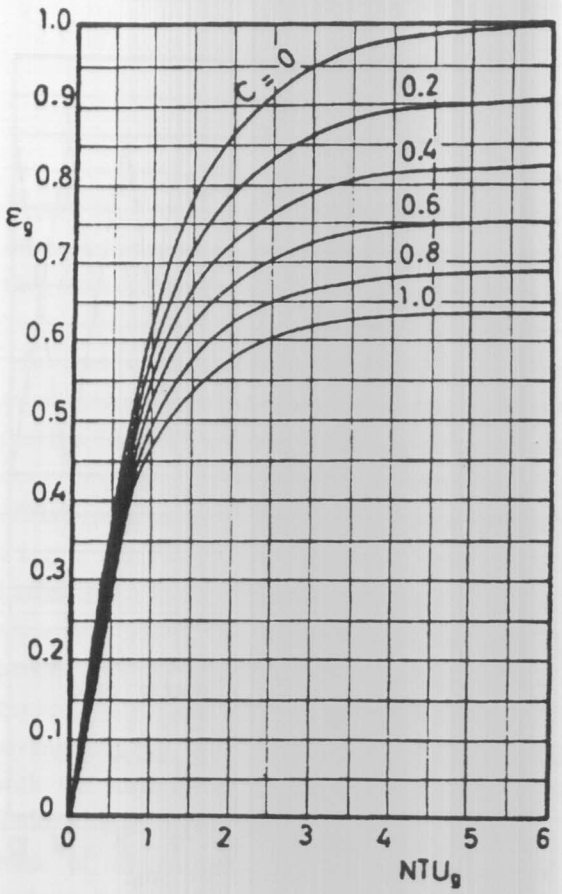

Figure 24. Variation of the grid effectiveness with the number of transfer units in the grid and the heat capacity rate ratio.

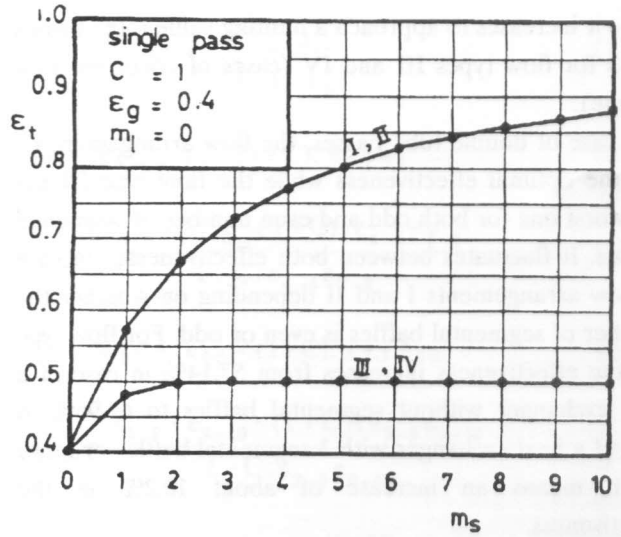

Figure 25. Dependence of the total effectiveness on the number of segmental baffles for different flow arrangements (single pass).

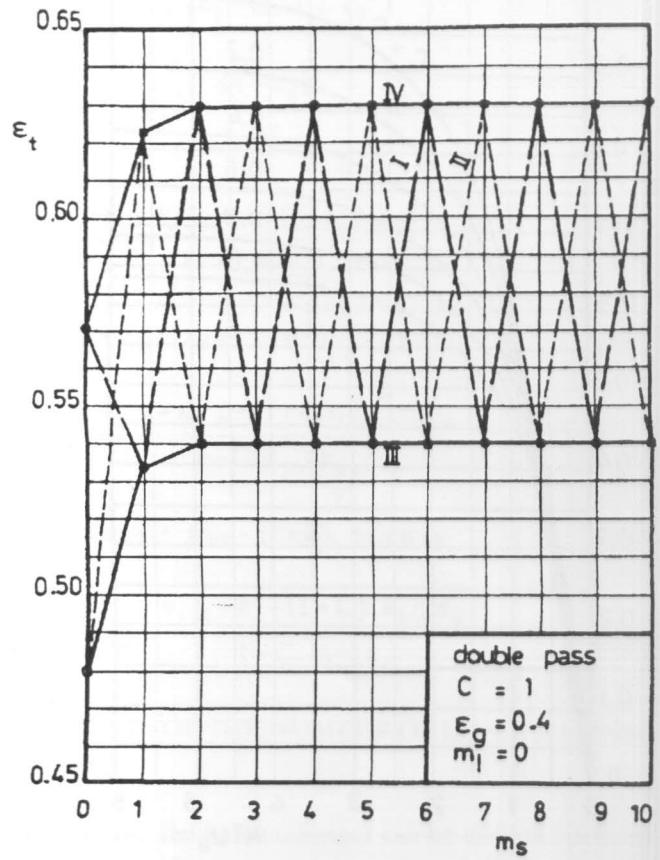

Figure 26. Dependence of the total effectiveness on the number of segmental baffles for different flow arrangements (double pass).

The total effectiveness of heat exchangers without longitudinal baffles is represented for both cases of a single pass and double passes as a function of the number of segmental baffles m_s and the heat capacity rate ratio C with $\varepsilon_g = 0.2$ in Figure (27) for flow type I and in Figure (30) for flow type IV. The same representation is done also for flow arrangement I in Figures (28 and 29) as well as for flow arrangement IV in Figures (31 and 32) with $\varepsilon_g = 0.4$ and 0.6 respectively. It can be easily seen that the effectiveness increases with the number of segmental baffles for a single tube pass to approach unity in case of flow type I (counterflow) and limiting values less than unity in case of flow type IV (parallel flow) depending on C (2/3 for C=0.5 and 0.5 for C=1). The effectiveness of both flow arrangements I and IV are equal when C=0 (case of evaporation or condensation). It is of interest to notice that when the grid (cell) effectiveness is higher than the limiting value the heat exchanger effectiveness decreases with m_s and fluctuates about the limiting value to approach it again (see Figure (32), for p=1 and C=1).

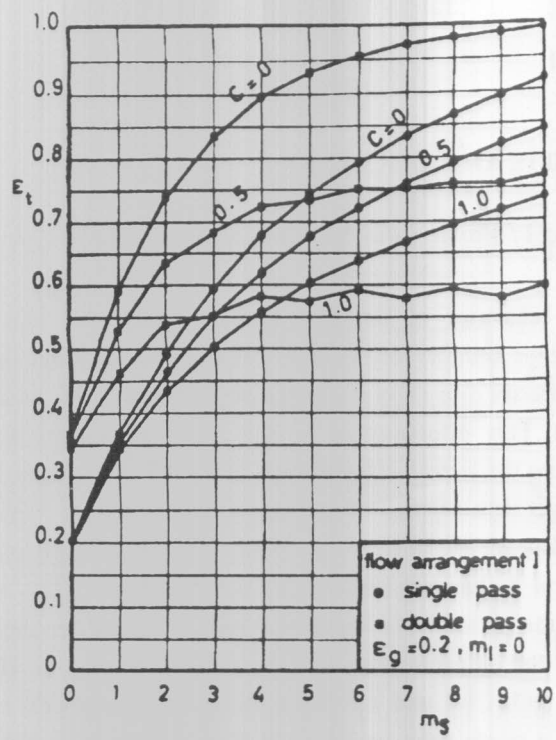

Figure 27. The heat exchanger effectiveness as a function of the number of segmental baffles and the heat capacity rate ratio for flow arrangement I, with ε_g = 0.2.

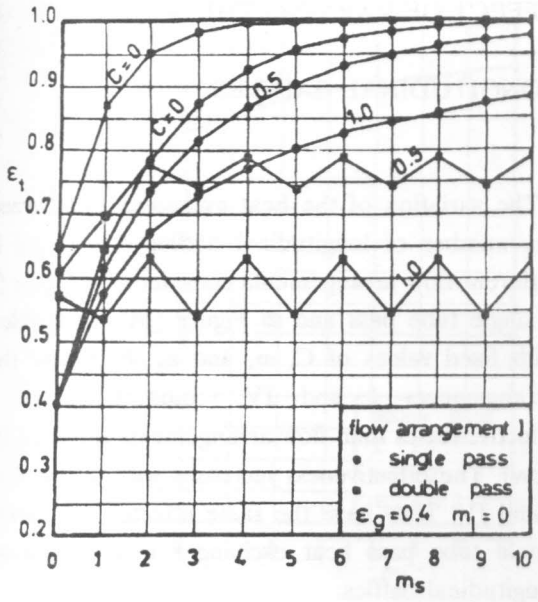

gure 28. The heat exchanger effectiveness as a function the number of segmental baffles and the heat capacity te ratio for flow arrangement I, with ε_g = 0.4.

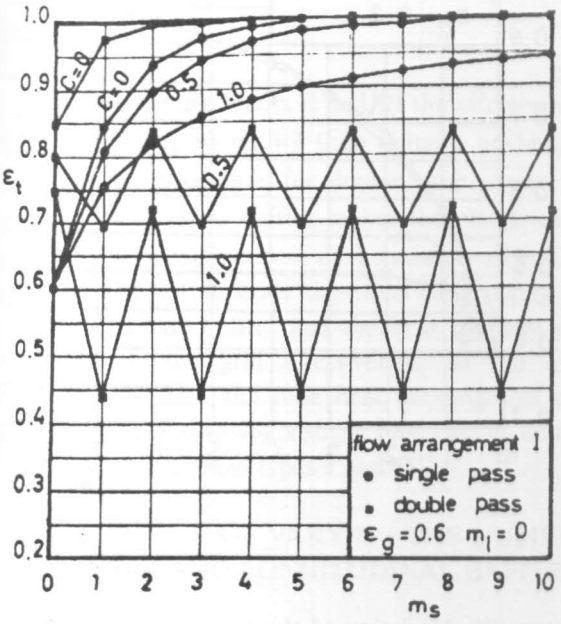

ure 29. The heat exchanger effectiveness as a function he number of segmental baffles and the heat capacity ratio for flow arrangement I, with ε_g = 0.6.

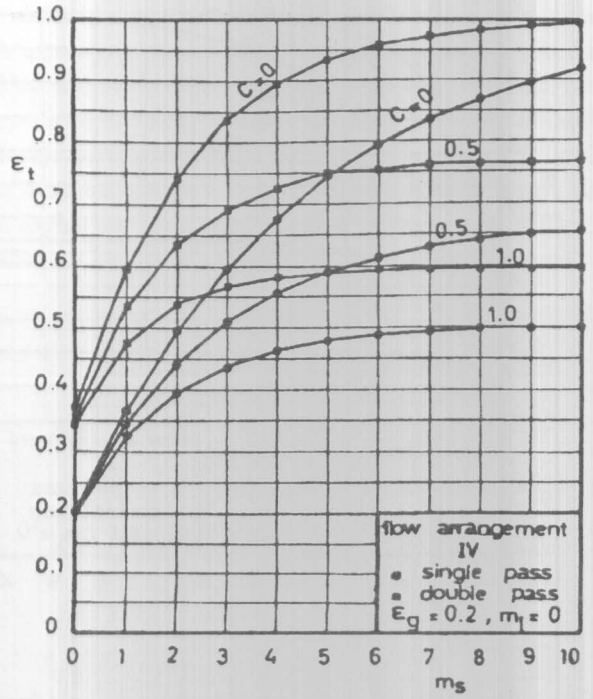

Figure 30. The heat exchanger effectiveness as a function of the number of segmental baffles and the heat capacity rate ratio for flow arrangement IV, with ε_g = 0.2.

In case of double tube passes, the heat exchanger effectiveness increases always with m_s for C=0 until it reaches unity at a certain number of segmental baffles depending on ε_g. For flow arrangement I and C>0, the effectiveness starts to fluctuate between two fixed values, a higher effectiveness in case of even number of segmental baffles and a lower effectiveness in case of odd number of segmental baffles. The difference between these two values becomes higher and higher with increasing both the heat capacity rate ratio and the grid effectiveness. For flow arrangement IV, the heat exchanger effectiveness increases with the number of segmental baffles to approach a limiting value depending on C and ε_g. When the starting value of effectiveness (i.e. the effectiveness of a heat exchanger without segmental baffles) is higher than the limiting value, the effectiveness decreases to reach the limiting value and then remains unchanged (see Figure (32), for p=2 and C=1).

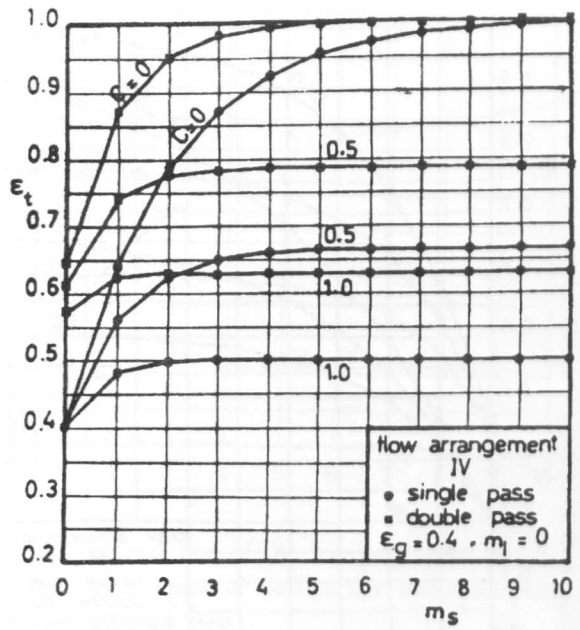

Figure 31. The heat exchanger effectiveness as a function of the number of segmental baffles and the heat capacity rate ratio for flow arrangement IV, with ε_g = 0.4.

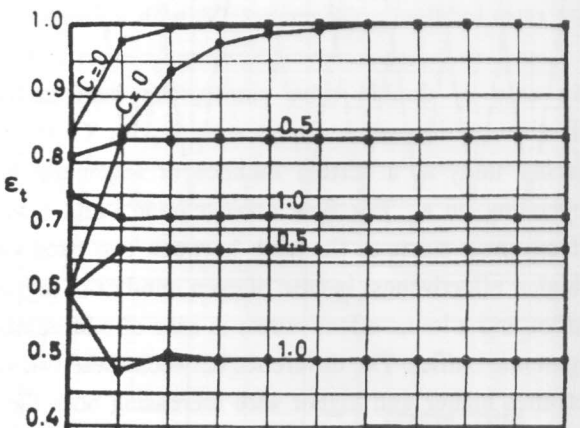

Figure 32. The heat exchanger effectiveness as a function of the number of segmental baffles and the heat capacity rate ratio for flow arrangement IV, with ε_g = 0.6.

EFFECT OF VARYING THE NUMBER OF LONGITUDINAL BAFFLES

The variation of the heat exchanger effectiveness with the number of longitudinal baffles is indicated for the different flow arrangements considered in Figure (33) for a single tube pass and in Figure (34) for double passes with fixed values of C, m_s and ε_g. It is clear that flow arrangements I and IV (counterflow) has higher effectivenesses than flow arrangements II and III (parallel flow). The effectiveness increases with m_l for flow types I and IV. They have the same effectiveness except for a single tube pass heat exchanger with even number of longitudinal baffles.

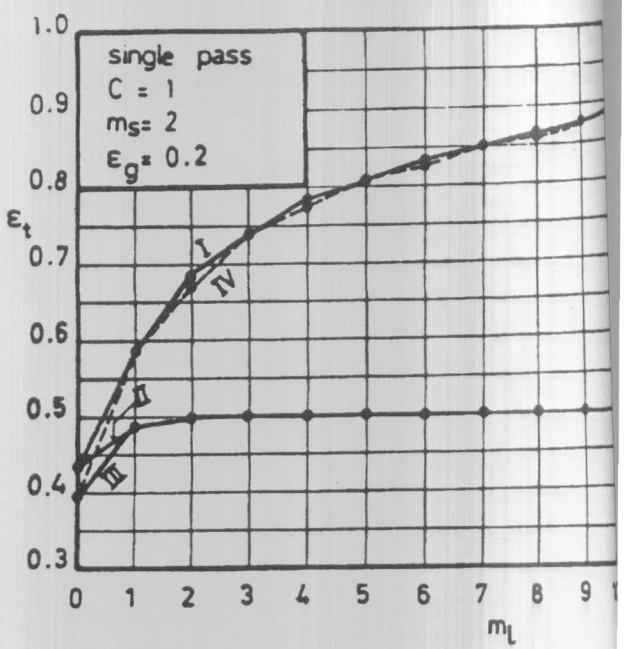

Figure 33. Variation of the heat exchanger effectiveness with the number of longitudinal baffles for the different flow arrangements, in case of a single tube pass heat exchanger.

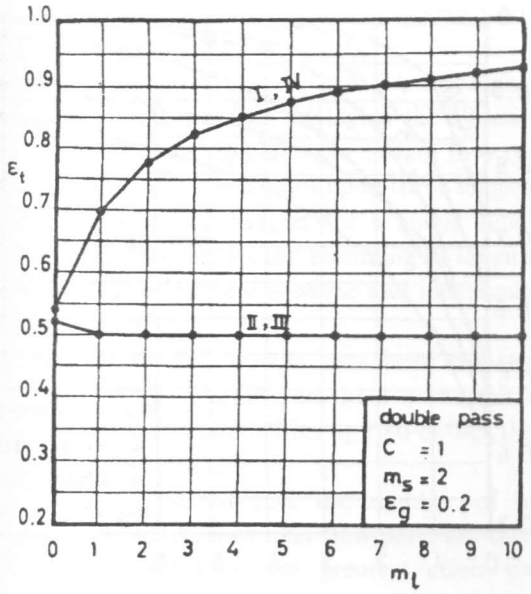

Figure 34. Variation of the heat exchanger effectiveness with the number of longitudinal baffles for the different flow arrangements, in case of a double tube pass heat exchanger.

In case of flow arrangements II and III the effectiveness increases with m_l up to m_l =3 then remains unchanged for a single tube pass while for double tube passes the mounting of longitudinal baffles makes the effectiveness worse and it will be independent of the number of baffles.

Figures (35 and 36) illustrate the effect of changing the number of segmental baffles and the heat capacity rate ratio as well as the grid effectiveness on the total effectiveness of a shell and tube heat exchanger of one longitudinal baffle and having a single tube pass or double tube passes in case of flow types I and IV.

COMBINED EFFECT OF VARYING THE NUMBER OF SEGMENTAL AND LONGITUDINAL BAFFLES

To show the combined effect of varying the number of longitudinal and segmental baffles as well as the heat capacity rate ratio in both cases of a single tube pass and double tube passes on the total effectiveness of tube bundles for a selected flow arrangement I (the optimum case) and a grid effectiveness ε_g = 0.2, Figures (37)-(39) are plotted.

It should be noted that the total effectiveness increases with increasing the number of segmental and longitudinal baffles and with decreasing the heat capacity rate ratio. The rate of increase is higher for small number of baffles and vice versa. Moreover, the effectiveness of a double pass heat exchanger is higher than that of a single pass heat exchanger for a small number of segmental baffles up to about 6 baffles then we have the other way round.

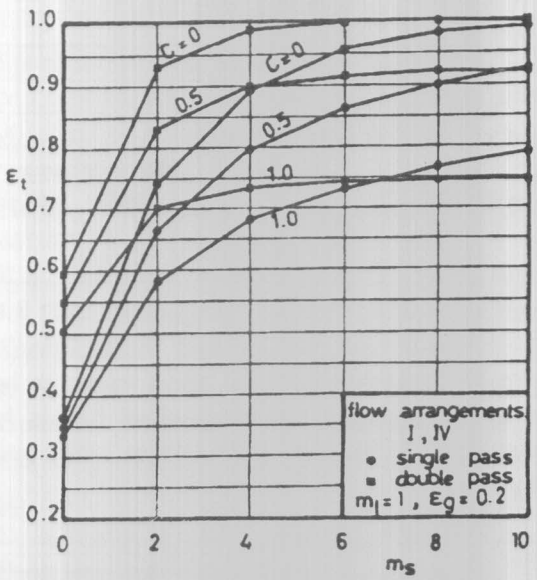

Figure 35. Variation of ε_t with m_s and C for m_l = 1 and ε_g = 0.2, in case of flow arrangements I and IV.

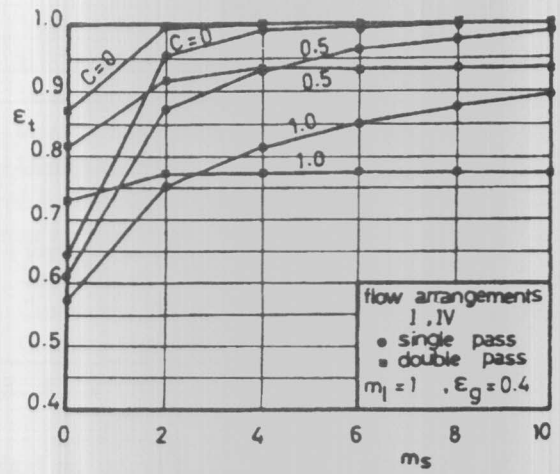

Figure 36. Variation of ε_t with m_s and C for m_l = 1 and ε_g = 0.4, in case of flow arrangements I and IV.

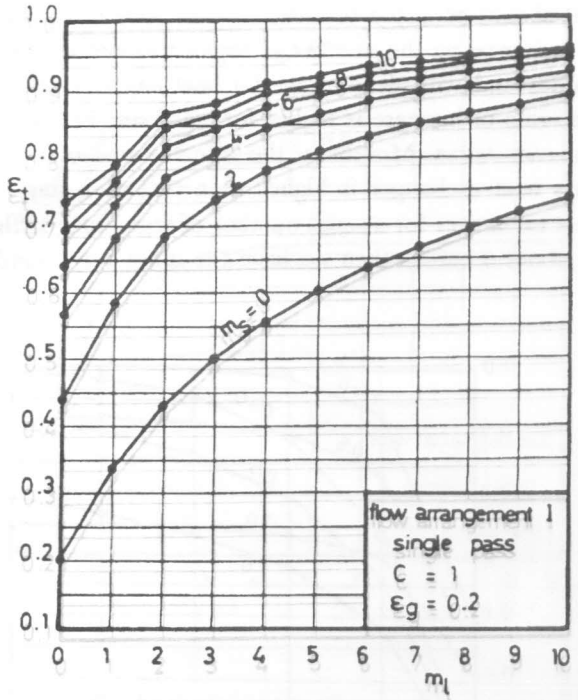

Figure 37. Dependence of the effectiveness on both the number of segmental and longitudinal baffles for flow arrangement I, in case of a single tube pass heat exchanger.

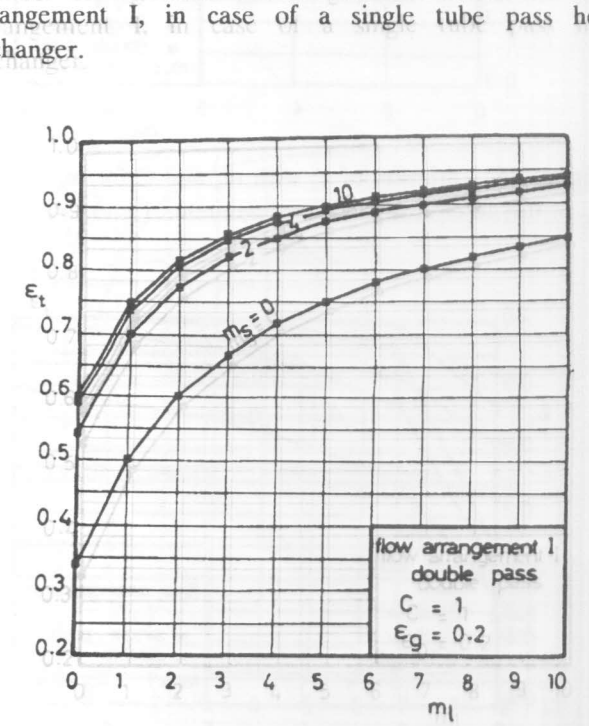

Figure 38. Dependence of the effectiveness on both the number of segmental and longitudinal baffles for flow arrangement I, in case of a double tube pass heat exchanger.

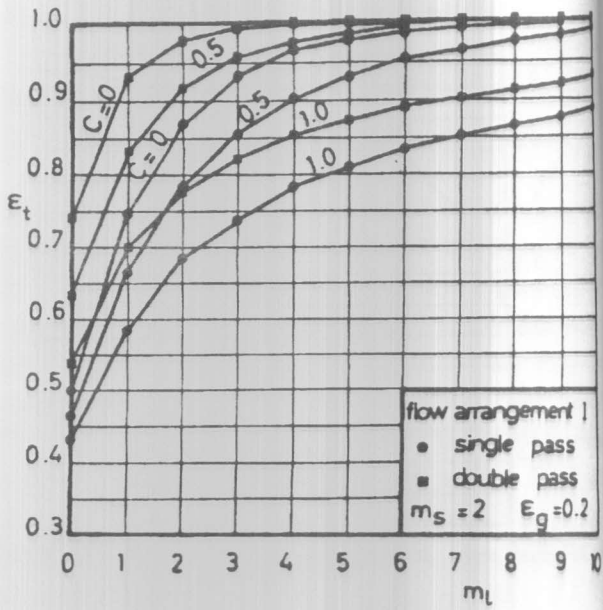

Figure 39. ε_t as a function of m_t and C with $m_s = 2$ and $\varepsilon_g = .2$, in case of flow arrangement I.

CONCLUSIONS

This paper deals with a study of the heat transfer behaviour in shell and tube heat exchangers under varying the number of segmental and longitudinal baffles on the shell side as well as the number of tube passes. The analysis is also carried out for all possible arrangements of the inlet flow ports with different values of the heat capacity rate ratio and the grid effectiveness. Thereby, the heat exchanger is divided at the location of baffles into a set of grids or cells each of which is handled as an inferior heat exchanger with crossflow. The number of these grids depends on both the number of baffles and the number of tube passes. The prediction of the overall effectiveness of the whole shell and tube heat exchanger becomes the possible through combining the sub-heat exchangers together in cocurrent or counter-current flow regimes.

It is shown that the overall effectiveness increases with increasing the number of segmental baffles for counterflow while it increases to approach a limiting value (50%) for heat exchangers of three or more segmental baffles for parallel flow. In case of double tube passes, the flow arrangement IV has the optimal effectiveness while the flow type III has the worst one for both odd and even number of segmental baffles. It fluctuates between both values in case of flow arrangements I and II depending on whether the number of baffles is odd or even. The difference between these two values becomes higher as

higher with increasing both the heat capacity rate ratio and the grid effectiveness.

Furthermore, for flow types I and IV, the higher the number of longitudinal baffles the higher the effectiveness of shell and tube heat exchangers. In case of flow types II and III, the effectiveness increases up to three longitudinal baffles then remains unchanged for a single tube pass while for double tube passes the mounting of longitudinal baffles makes the effectiveness worse and independent of the number of baffles.

The effectiveness of a double pass heat exchanger is higher than that of a single pass heat exchanger for a small number of segmental baffles up to 6 baffles then we have the other way round.

Finally, it can be stated that the number of baffles together with the location of inlet flow ports are the most relevant factors that have the greatest effect on the effectiveness of a shell and tube heat exchanger. Therefore, careful consideration should be given to the selection of the number of baffles and the type of flow arrangement.

NOMENCLATURE

C	heat capacity rate ratio
m_t	number of longitudinal baffles
m_s	number of segmental baffles
NTU	number of transfer units
p	number of passes

Greek symbols:

ε	effectiveness

Subscripts:

g	grid (cell)
I	flow arrangement I
II	flow arrangement II
III	flow arrangement III
IV	flow arrangement IV
t	total

REFERENCES

[1] N.H. Afgan and E.U. Schlünder, *Heat Exchangers Design and Theory Source Book*, McGraw-Hill Book Company, New York, 1974.

[2] S. Kakac, A.E. Bergles and F. Mayinger, *Heat Exchangers - Thermohydraulic Fundamentals and Design*; Hemisphere Publishing Corp.,New York, 1981.

[3] R.C. Lord, P.E. Minton and R.P. Slusser, "Design of Heat Exchangers", Heat Exchanger Design and Specification, Jan. 26, 1970, pp. 14-36.

[4] M.D. Mikhailov and M.N. Ozisik, *Finite Element Analysis of Heat Exchangers*; in Heat Exchangers-Thermohydraulic Fundamentals and Design; Hemisphere Publishing Corp., New York, 1981, pp. 461-479.

[5] R.K. Hoffmann, "How to Find the Optimum Layout for Heat Exchangers"; *Heat Exchanger Design and Specification*, Sept. 12, 1977, pp. 79-88.

[6] J. Fanaritis and J. Bevevino, "How to Select the Optimum Shell-and-Tube Heat Exchanger"; *Heat Exchanger Design and Specification*, July 5, 1976, pp. 5-13.

[7] D. Butterworth and L. Cousins, "Use of Computer Programs in Heat-Exchanger Design"; *Heat Exchanger Design and Specification*, July 5, 1976, pp. 109-113.

[8] W.M. Kays and A.L. London, *Compact Heat Exchangers*, McGraw-Hill Book Company, New York, 1984.

[9] E. Gaddis and A. Vogelpohl, "Über den Wirkungsgrad und die mittlere Temperaturdifferenz von Rohrbundelwärmeübertragern mit Umlenksegmenten und zwei rohrseitigen Gängen", *Chem. Eng. Process*, Vol. 18, 1984, pp. 269-273.

[10] M.K. Bassiouny, "Performance Prediction of Heat Exchangers; Part I: Performance of In-Series Connected Heat Exchangers with Cocurrent and Counter-Current Flow Regimes; *This issue*.